ICES Journal of Marine Science (2011), 68(3), 626–631. doi:10.1093/icesjms/fsq172

Real-time calibration of *in situ* measurements of target strength

David N. MacLennan*

The Orchard, Muirhall Road, Perth PH2 7BQ, Scotland, UK

**Corresponding Author: tel/fax: +44 1738 444090; e-mail: maclennan22@aol.com.*

MacLennan, D. N. 2011. Real-time calibration of *in situ* measurements of target strength. – ICES Journal of Marine Science, 68: 626–631.

Received 25 June 2010; accepted 14 October 2010; advance access publication 22 December 2010.

The *in situ* measurement of target strength (*TS*) depends on exactly one fish being within the sampled volume. This is more likely to occur the nearer the transducer is to the fish targets. The detection rate can be improved by lowering the transducer on a cable from a stationary vessel, so decreasing the range to the observed fish. In this application, a standard sphere is commonly suspended below the transducer to provide the real-time calibration of the received signals. However, forward scattering by the sphere distorts the transmitted pulse, and equally the returning fish echoes, causing a bias in the estimated *TS*. Further, for a split-beam transducer, forward-scattering of the fish echo by the sphere modifies the phase differences observed between the transducer segments. This changes the apparent distribution of targets, but not the estimated *TS*. The biases are not large, those considered being within ± 0.9 dB, and they depend on the sonar frequency, the target range, and the direction. The theory of these effects is examined, and formulae are provided for correcting the observed fish echo to that which would be received in free-field conditions, i.e. with the sphere removed.

Keywords: acoustic calibration, forward-scattering, split-beam transducer, target strength.

Introduction

The accurate measurement of fish target strength (*TS*) is essential for the useful interpretation of acoustic surveys of fish stocks (Simmonds and MacLennan, 2005). This is best done by *in situ* methods where the fish are observed in their natural state. A split-beam echosounder is commonly used for this purpose (Carlson and Jackson, 1980). This instrument transmits a short sinusoidal pulse, and phase differences in the signals received across the transducer face are used to determine the target direction, and hence to compensate for the directional dependence of the transducer sensitivity, i.e. the beam pattern.

The measured *TS* is only valid when exactly one fish is detected inside the sampled volume. This is a truncated cone bounded vertically by the pulse length and horizontally by the beam width, so the sampled volume increases with the range of the target. This limits the *TS* data available to near-surface transducers mounted on vessels. Alternatively, the transducer can be lowered on a cable from a stationary vessel or other platform, so decreasing the range to the target fish and increasing the rate of single-fish detections (Kloser *et al.*, 2009). In this method, a sphere of known *TS* is often deployed below the transducer to provide real-time calibration signals, allowing effects such as depth-dependence or other environmental effects on transducer sensitivity to be accurately compensated for. Spheres made from tungsten carbide or copper, whose scattering properties are well understood, are commonly used for the purpose (Foote and MacLennan, 1984).

The presence of the sphere, however, distorts the acoustic fields of both outward transmission and returning echoes, because the sphere scatters acoustic waves in all directions. The theory of acoustic scattering by a homogeneous solid sphere is well established and allows precise calculation of the scattered wave (Hickling, 1962; MacLennan, 1982). In the present context, the backscattered wave, i.e. the sphere echo, is the calibration signal. This is undistorted because it is received at times different from the echoes of fish assumed to be deeper than a pulse length below the sphere. However, the scattering in forward directions close to that of the incident wave at the sphere is largely coincident with the transmitted pulse, and has consequent effects on the amplitude and phase of the incident signal at the fish. The returning fish echoes are subject to similar distortions, which increase the effect on the signals received at the transducer. Further, for split-beam transducers, which depend on phase differences to determine target direction, there is an additional effect, because the apparent direction of the fish is altered by the forward-scattering of its echo.

Here, the theory of these effects is explained and an attempt made to show how the observed *TS* and fish distributions can be corrected to remove the bias caused by the forward-scattering properties of the calibration sphere.

Theory

When a single target is detected by a sonar, the echo intensity (I) is proportional to σ_{bs}, the backscattering cross section of the target. With appropriate corrections for spreading losses and beam directivity, measurements of I determine the *TS* in dB through the formula $TS = 10\log_{10}(\sigma_{bs})$. For the basic theory of fishery applications in underwater acoustics, see Simmonds and MacLennan (2005).

Figure 1 illustrates the geometry in the fish–sphere–transducer plane when a calibration sphere is positioned at range R_1 below the transducer on the acoustic axis, the direction of maximum sensitivity in the beam pattern. A fish is detected at range R_2 and angle θ off axis. D is the distance of the fish from the sphere. In reality, the fish is located in three dimensions by the measurement of its range and two angles relative to the transducer axes. However, these angles uniquely determine θ, which is the key parameter in the

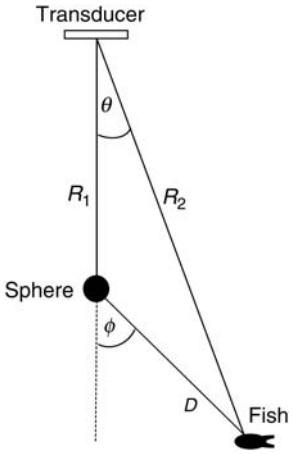

Figure 1. Geometry of a real-time calibration system. The calibration sphere is located at range R_1 on the acoustic axis below the transducer by suspension wires, not shown in the diagram. The observed fish is at range $R_2 > R_1$. Both the outward transmission and the returning fish echo are influenced by the forward-scattering properties of the sphere.

present study, and only the two-dimensional geometry in the above-mentioned plane is relevant here.

The sonar transmits a sinusoidal pulse, which has constant amplitude at frequency ω and duration τ and which is assumed to be long enough for continuous-wave solutions to apply around the midpoint of the pulse. The transmitted pulse is first incident upon the sphere and later arrives at the fish. In the meantime, a forward-scattered pulse emanates from the sphere. This combines with the transmission and alters the pulse incident on the fish.

The sound-pressure amplitude from any one source is described by

$$P = P_0(r)\,\exp[i(\omega t - kr)], \tag{1}$$

where r is the range from the source, t the time after the transmission (restricted to times around the midpoint of the pulse at range r), k the wave number, i.e. 2π divided by the wavelength, and $i = \sqrt{(-1)}$. In this notation, P is the complex amplitude, which indicates both the signal amplitude at range r, as the real quantity $P_0(r) = |P|$, and the signal phase from the ratio of the real and imaginary parts of P.

If R_1 and D are large enough for far-field conditions to apply, the direct transmissions incident upon the sphere (subscript S) and the fish (subscript F) are described by

$$P_s = \left(\frac{G}{R_1}\right)\exp[i(\omega t - kR_1)], \tag{2}$$

$$P_{\mathrm{F}} = \left(\frac{G}{R_2}\right)\exp[i(\omega t - kR_2)], \tag{3}$$

where G is a constant that depends on the transmitted power. The forward-scattered wave at the fish is

$$P_{\mathrm{fwd}} = \left(\frac{G}{R_1}\right)\left(\frac{a}{2D}\right)F(\phi)\,\exp\,[i(\omega t - k\{R_1 + D\})], \tag{4}$$

where a is the sphere radius, F the so-called form function that describes the scattering properties of the sphere, and ϕ is the angle of the sphere–fish line off the acoustic axis. In addition to ϕ, F depends on various physical parameters, which are constants in a given application. These are the sonar frequency ω, the sound-speed ratios c_1/c and c_2/c, and the density ratio ρ_1/ρ. Here, c_1 and c_2 are the longitudinal and transverse sound speeds within the sphere, respectively, ρ_1 is the sphere density, and c and ρ are, respectively, the sound speed and the density in the surrounding water.

If θ and ϕ are small, the forward-scattered and direct pulses largely overlap, and the incident pulse at the fish is $P_{\mathrm{F}} + P_{\mathrm{fwd}}$. Exactly the same forward-scatter interference applies to the returning fish echo, so the received amplitude at the transducer is proportional, by a factor depending only on the sphere and target positions, to $(P_{\mathrm{F}} + P_{\mathrm{fwd}})^2$. The echo intensity is the modulus of the amplitude squared. If I_0 is the intensity that would be received without a calibration sphere ($P_{\mathrm{fwd}} = 0$), then

$$\frac{I}{I_0} = \left|1 + \frac{P_{\mathrm{fwd}}}{P_{\mathrm{F}}}\right|^4 = \left|1 + \left[\frac{aF(\phi)R_2}{2DR_1}\right]\exp[-ik(R_1 + D - R_2)]\right|^4. \tag{5}$$

The explicit time-dependence $\exp(i\omega t)$ has cancelled in the above ratio. The numerical evaluation of Equation (5) requires the following geometric relationships:

$$D = \sqrt{R_1^2 + R_2^2 - 2R_1R_2\cos\,\theta}, \tag{6}$$

$$\sin\,\phi = \left(\frac{R_2}{D}\right)\sin\,\theta. \tag{7}$$

Therefore, Equations (5)–(7) determine the correction factor that should be applied to the measured intensities around the middle of largely overlapping pulses to compensate for the forward-scattering interference introduced by the sphere, assuming that the measurements are compensated for the beam pattern. The corresponding error in the estimated *TS* would then be $10\log_{10}(I/I_0)$.

Equation (5) is simplified by writing $F(\phi) = |F(\phi)|\exp(i\beta)$, where $|F(\phi)|$ is the modulus and β the phase shift associated with the form function. Also, by defining the real parameters h and γ as

$$h = \frac{a|F(\phi)|R_2}{2DR_1}, \tag{8}$$

$$\gamma = \beta - k(R_1 + D - R_2), \tag{9}$$

combining Equations (5), (8), and (9) and evaluating the modulus in Equation (5) gives the simpler expression

$$\frac{I}{I_0} = [1 + 2h\,\cos\,\gamma + h^2]^2. \tag{10}$$

As $-1 < \cos\,\gamma < +1$, it follows from Equation (10) that I/I_0 is bounded by the range $(1-h)^4$ to $(1+h)^4$. Therefore, the correction factor can be greater or less than 1, depending on the geometry and phase shifts.

When a split-beam transducer is used, the target direction θ is assumed to be determined by phase differences in the signals received across the transducer face. The beam pattern as a function of θ is assumed to be known from other calibration procedures. In three-dimensional geometry, the beam pattern of an asymmetrical transducer will vary with the azimuthal angle, but that is not relevant in the present context. The point is that in the fish–sphere–transducer plane, the apparent target angle θ_a differs from the true angle θ as a result of the forward-scattering of the fish echo. Only one-way transmission, on the echo-return paths, the direct one and that via the sphere, is relevant to this part of the analysis. With the sphere on the acoustic axis, the forward-scattered fish echo has zero phase difference. This combines with the direct echo returned from the fish at angle θ, altering the observed phase difference and hence the apparent target direction. The beam pattern is still correctly compensated in the receiver, so the measured intensities and the estimated *TS* values are not affected. This effect is only important if the spatial distribution of targets within the beam is being considered. In that case, the target directions may need to be compensated for the forward-scatter interference.

Let $2d$ be the distance between two phase-measurement points on the transducer face which are equidistant from the transducer centre. The direct echo from the fish at these points is proportional to P_F multiplied by $\exp(-ikd \sin\theta)$ and $\exp(ikd \sin\theta)$, respectively. The ratio of these two signals is $\exp(-2\,ikd \sin\theta)$ and, with no sphere present, this ratio determines the target direction θ in the fish–sphere–transducer plane. However, the sphere adds P_{fwd} to each signal with no phase shift. The ratio (R) of the combined amplitudes at the two phase-measurement points is now

$$R = \frac{P_{fwd} + P_F \exp(-ikd \sin\theta)}{P_{fwd} + P_F \exp(ikd \sin\theta)}, \quad (11)$$

which is interpreted by the sonar as $|R| \exp(-2ikd \sin\theta_a)$, giving an apparent target direction θ_a that in general is different from θ. An approximate small-angle solution valid for $\theta << 1$ radian (57.3°) is presented here. Combining Equations (3), (4), (8), (9), and (11), and ignoring terms in θ^2 or higher powers, the small-angle correction formula is

$$\theta_a = \frac{\theta(1 + h \cos\gamma)}{1 + 2h \cos\gamma + h^2}. \quad (12)$$

The transducer-dependent distance d does not appear in Equation (12) because it cancels in the first-order approximation. Note that θ_a could be greater or less than θ, depending on the value of $\cos\gamma$. The ratio θ_a/θ is bounded by the range $1/(1 + h)$ to $1/(1 - h)$.

Results

Some calculations are presented here as examples relating to the 38.1-mm-diameter, tungsten carbide sphere. This is a standard target commonly used to calibrate fishery sonars operating in the frequency range 38–120 kHz (Foote and MacLennan, 1984; Foote *et al.*, 1987). The acoustic properties of this sphere are detailed in Table 1 (after MacLennan and Dunn, 1984).

Figure 2 shows the modulus F and the phase $\beta = \arg(F)$ of the form function for angles ϕ from 0 to 10° off the acoustic axis for three frequencies, 38, 70, and 120 kHz. The formulae for calculating F are in Hickling (1962) and MacLennan (1982). The forward-scattering by the sphere is strongly dependent on the frequency. $|F|$ increases and the phase β reduces with the frequency. Clearly, the effect on the observed echo intensity is more severe at the higher frequencies.

Table 1. Physical properties of the 38.1-mm, tungsten carbide calibration sphere, where c_1 and c_2 are, respectively, the longitudinal and transverse sound speeds within the sphere (after MacLennan and Dunn, 1984).

Property	Value
Radius (a, mm)	19.05
Density (ρ_1, kg m^{-3})	14 900
c_1 (m s^{-1})	6 853
c_2 (m s^{-1})	4 171

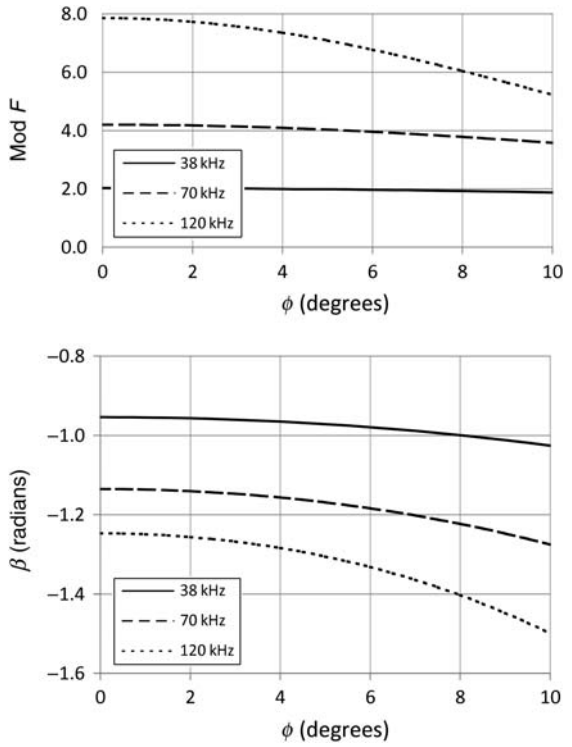

Figure 2. Forward-scattering properties of a tungsten carbide calibration sphere, 38.1 mm in diameter. The form function is $F = |F| \exp(i\,\beta)$. (Top panel) modulus F; (bottom panel) phase angle β. Results are shown for three frequencies and off-axis angles out to 10°.

The forward-scattered and direct transmissions combine with constructive or destructive interference depending on the fish direction θ. The signal processing in a split-beam sonar normally limits the single-fish detections to targets near the acoustic axis, and typically $\theta = 5°$ would be the maximum considered. Suppose the sphere is suspended at $R_1 = 5$ m below the transducer. For this geometry, the total effect of forward-scattering on the echo intensity from near-axis targets is shown in Figure 3, for the same three frequencies and target ranges of 7 m, 20 m, and infinity. The constructive/destructive interference causes cyclic changes with target direction, which are strongest at the shortest range and increase with the frequency. The maximum corrections required to the observed echo intensity for targets at 7 m

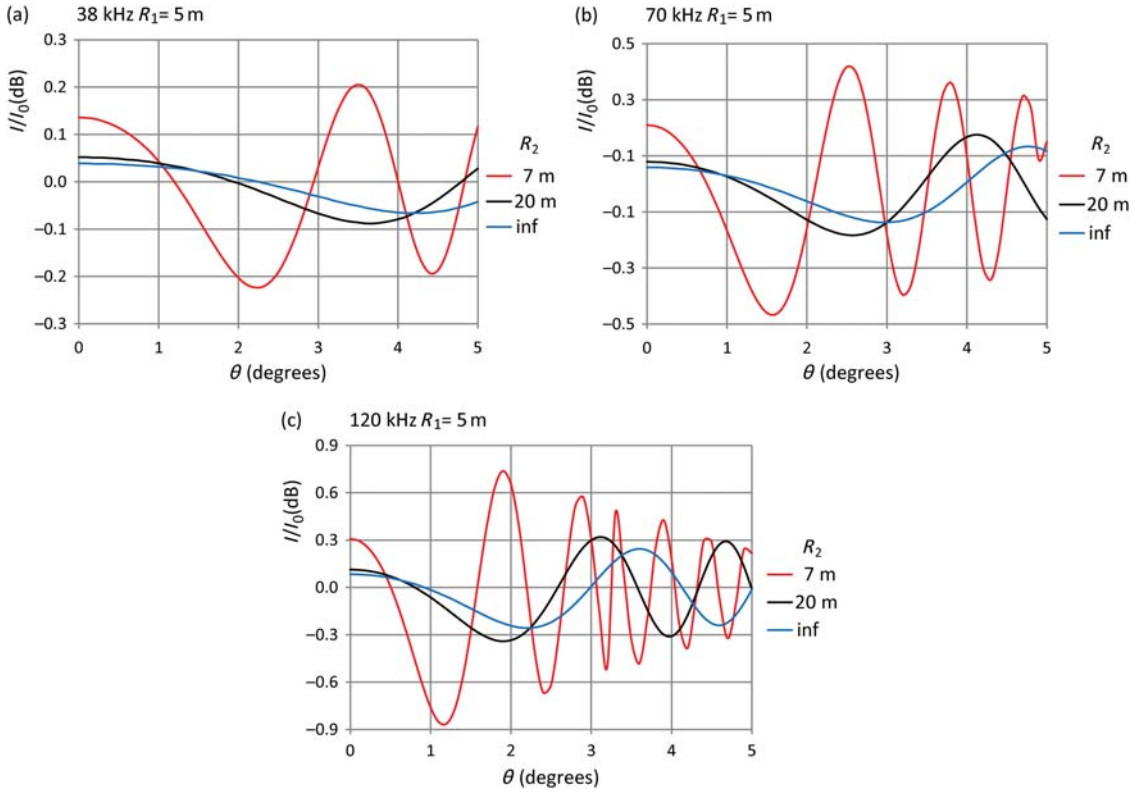

Figure 3. The factor I/I_0 that corrects observed echo intensities from single-fish targets for the forward-scattering interference by a 38.1-mm, tungsten carbide calibration sphere 5 m below the transducer. Results for a fish at three ranges R_2 and off-axis angles θ out to 5°; inf, very large or infinity. Panels are labelled with the acoustic frequency: 38, 70, or 120 kHz.

range, with the sphere present, are around ± 0.2, 0.4, and 0.8 dB at 38, 70, and 120 kHz, respectively.

Figure 4 shows additional examples, in this case with the fish at a constant 20 m range and the sphere at $R_1 = 5$, 10, or 15 m. For each frequency, the maximum errors are similar, although the cyclic variation with θ is more rapid at the larger R_1.

The changes in the apparent target direction determined from Equation (11) are small. They are greatest at the shortest ranges ($R_1 = 5$ m, $R_2 = 7$ m) and the highest frequency (120 kHz), but even then are only some $\pm 0.1^\circ$ over the interval $\theta = 0$–5°. This appears to be a second-order effect that is unlikely to be important in the type of application considered here.

Discussion and conclusions

The real-time calibration of a fisheries sonar normally involves a standard sphere suspended below the transducer at shorter range than the observed fish. Forward scattering by the sphere interferes with the transmission and the returning fish echo, hence biasing the observed values of *TS* obtained from single-fish detections. Here, the theory of this effect has been explained and formulae presented to correct the bias. In typical applications, the bias increases with the sonar frequency and reduces with the range of the observed fish relative to that of the sphere.

It has been assumed in the analysis that the forward-scattered and directly transmitted waves largely overlap, so that continuous-wave solutions can be applied. These will be relevant to the superimposed pulses if they are long enough for the initial and the final transients to be negligible over several cycles around the middle of the signal. The more complicated interactions at the beginning and the end of combined pulses, which are not exactly coincident, have not been considered here. The worst case occurs at the shortest range and the widest angle ($R_1 = 5$ m, $R_2 = 7$ m, $\theta = 5^\circ$), when the non-overlapping sections at the start and the end of the combined pulse will be around 0.04 ms long. This is small compared with the typical 0.5 ms or longer pulses commonly used in practice. Therefore, it is reasonable to use continuous-wave solutions relevant to the middle of the received signals. However, note that if a phase-stability criterion is applied in the single-target detector, some targets might be rejected because of the variable phase at the start and the end of the received signals and that this is more likely with targets at the largest off-axis angles. Hence, the effective width of the acceptance cone might be reduced for short-range targets.

The analysis here has assumed negligible difference between fish echoes at the same range returned in the directions of the transducer and the sphere. The directional-scattering properties of fish are not well understood, at least in quantitative terms, so the validity of this assumption is uncertain. On the other hand, there is no reason to expect any substantial change in echo amplitude over the small range of angles being considered, i.e. $<10^\circ$ from the backscattering direction. Further work is required to quantify this effect, which will depend on fish size, orientation, and physiology.

The *TS* biases in the examples presented here are within ± 1 dB. This is not large compared with the spread of *TS* values normally shown by *in situ* experiments, e.g. Kloser and

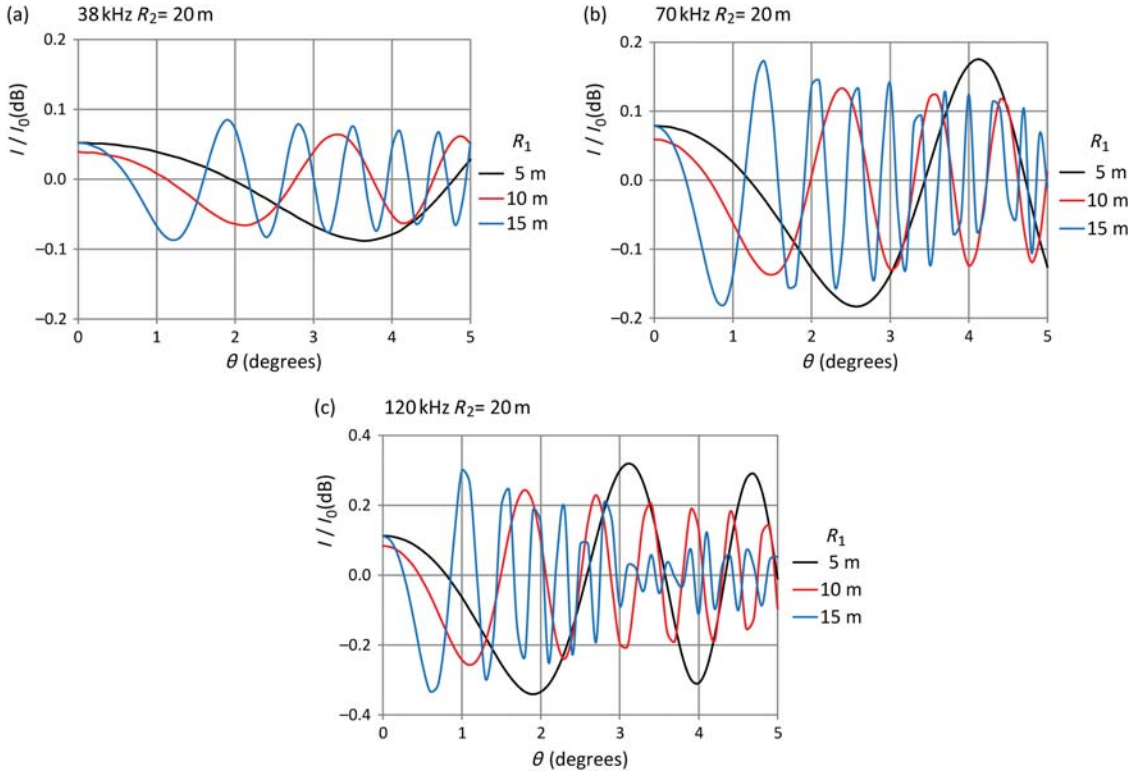

Figure 4. The factor I/I_0 that corrects observed echo intensities from single-fish targets for the forward-scattering interference by a 38.1-mm, tungsten carbide calibration sphere at $R_1 = 5$, 10, or 15 m below the transducer. Results are given for a fish at 20 m range and off-axis angles θ out to 5°. Panels are labelled with the acoustic frequency: 38, 70, or 120 kHz.

Horne (2003) and Rose (2009). Although the mean *TS* over many detections will be little affected, the variance of the results could be up to 1 dB more than the true value in the worst-case examples being considered. Suspending the sphere deeper below the transducer, e.g. at 10 m instead of 5 m, is an option that reduces the worst-case bias. Nevertheless, good scientific practice suggests that the forward-scatter bias be removed before the results are presented. It is not difficult to do this, because the data required are already available from the spatial location of the detected targets.

This study focused on signal distortion caused by the forward-scatter from a calibration sphere. Similar distortions will be introduced by any target that is between the detected fish and the transducer. Therefore, when a diffuse fish layer is being investigated, echoes from fish near the bottom of the layer will be distorted by forward-scattering via any other fish that are higher in the water column, but within the detection cone. If there are many fish between the target and the receiver, multiple scattering (see Stanton, 1983, 1984; Furusawa *et al.*, 1992) could further complicate matters.

In situ TS measurements made in the presence of multiple scatterers are liable to distortions even if single-target criteria are satisfied. Obviously, the best results will be obtained with the observed fish in empty water, but that is seldom attainable in practice. Hence, there is scope for further work on the reliability of *in situ TS* measurements which could be compromised by the presence of biological targets near the transmission paths, in the same way as has been demonstrated in this paper for the simpler case of a single calibration sphere.

References

Carlson, T. J., and Jackson, T. R. 1980. Empirical evaluation of split-beam methods for direct *in-situ* target strength measurement of single fish. Seattle Applied Physics Laboratory, University of Washington. 43 pp.

Foote, K. G., Knudsen, H. P., Vestnes, G., MacLennan, D. N., and Simmonds, E. J. 1987. Calibration of acoustic instruments for fish density estimation: a practical guide. ICES Cooperative Research Report, 144. 57 pp.

Foote, K. G., and MacLennan, D. N. 1984. Comparison of copper and tungsten carbide calibration spheres. Journal of the Acoustical Society of America, 75: 612–616.

Furusawa, M., Ishii, K., and Miyanohana, Y. 1992. Attenuation of sound by schooling fish. Journal of the Acoustical Society of America, 92: 987–994.

Hickling, R. 1962. Analysis of echoes from a solid elastic sphere in water. Journal of the Acoustical Society of America, 34: 1582–1592.

Kloser, R. J., and Horne, J. K. 2003. Characterizing uncertainty in target-strength measurements of a deepwater fish: orange roughy (*Hoplostethus atlanticus*). ICES Journal of Marine Science, 60: 516–523.

Kloser, R. J., Ryan, T. E., Young, J. W., and Lewis, M. F. 2009. Acoustic observations of micronekton fish on the scale of an ocean basin: potential and challenges. ICES Journal of Marine Science, 66: 998–1006.

MacLennan, D. N. 1982. The theory of solid spheres as sonar calibration targets. Scottish Fisheries Research Report, 25. 17 pp.

MacLennan, D. N., and Dunn, J. 1984. Estimation of sound velocities from resonance measurements on tungsten carbide calibration spheres. Journal of Sound and Vibration, 97: 321–331.

Rose, G. A. 2009. Variations in the target strength of Atlantic cod during vertical migration. ICES Journal of Marine Science, 66: 1205–1211.

Simmonds, E. J., and MacLennan, D. N. 2005. Fisheries Acoustics, 2nd edn. Blackwell, Oxford. 437 pp.

Stanton, T. K. 1983. Multiple scattering with applications to fish-echo processing. Journal of the Acoustical Society of America, 73: 1164–1169.

Stanton, T. K. 1984. Effects of second-order scattering on high resolution sonars. Journal of the Acoustical Society of America, 76: 861–866.